Entropy-Heat Transfer Coupling in Vibrational Non-Newtonian Nanofluid Flow with two phase study

Amrita Tripure
UTD, Chhattisgarh Swami Vivekanand Technical University

Santosh Kumar Mishra
Bhilai Institute of Technology

Amrit Shende
UTD, Chhattisgarh Swami Vivekanand Technical University

Pushpendra Singh
Bhilai Institute of Technology

出版情報：Evergreen. 13 (2), pp.455-465, 2026-06. 九州大学グリーンテクノロジー研究教育センター
バージョン：

Entropy-Heat Transfer Coupling in Vibrational Non-Newtonian Nanofluid Flow with two phase study

Amrita Tripure[1], Santosh Kumar Mishra[2,*], Amrit Shende[1], Pushpendra Singh[2]

[1]UTD, Chhattisgarh Swami Vivekanand Technical University, Bhilai, Durg, CG, 491001, India
[2]Bhilai Institute of Technology, Durg, CG, 491001, India

*Author to whom correspondence should be addressed:
E-mail: san810@gmail.com

(Received June 24, 2025; Revised November 14, 2025; Accepted March 16, 2026)

Abstract: This study investigates the coupled effects of mechanical vibration on heat transfer and entropy generation in non-Newtonian nanofluid flow under constant wall temperature conditions. The introduction of vibration promotes radial mixing and temperature uniformity, leading to a marked increase in convective heat transfer. Parametric analysis reveals that amplitude is the most influential factor, followed by frequency, Reynolds number, and nanoparticle concentration. Increasing vibration amplitude consistently enhances the Nusselt number across all Reynolds numbers, with values rising from approximately 38–118 in the static case to 202–224 at 4 mm amplitude and 100 Hz. The frequency effect becomes more prominent at higher amplitudes, with optimal enhancement observed between 25–100 Hz. Entropy-based analysis shows that vibration reduces total irreversibility by mitigating thermal gradients; however, excessive vibration can elevate viscous dissipation, increasing entropy generation. Thus, optimal thermal performance is achieved at moderate amplitudes and relatively high frequencies, balancing enhanced heat transfer with minimized entropy production. Two-phase numerical modeling accurately captures nanoparticle slip, diffusion, and clustering effects, exhibiting better agreement with experimental data than single-phase models. The findings provide valuable insights for the design and optimization of nanofluid-based thermal systems operating under vibrational environments.

Keywords: Entropy Generation; Heat Transfer; Irreversibility; Volume of Fluid (VOF) Method

1. Introduction

Several techniques are used to enhance heat transfer performances since ages. These techniques are broadly classified into a). Active and b). Passive techniques. Rotation, mechanical mixing and vibration are techniques to active heat transfer enhancement that rely on external energy input. These methods work by altering the fluid's thermophysical properties, modifying the surface geometry with grooves or roughness, or inducing turbulence to improve convective efficiency. Among these techniques, mechanical vibration has attracted particular attention because it can actively promote both heat and mass transfer. Vibration may occur unintentionally in vehicular or marine systems or be deliberately introduced for industrial mixing and thermal regulation, and it is commonly classified as wall vibration, internal vibration, or system-wide vibration depending on its mode of application.

A wide range of studies have demonstrated the thermal benefits of vibration in engineering systems. On experimental examination the performance of automotive heat exchangers under vibration and found that increasing vibration amplitude and frequency enhanced heat-transfer efficiency[1)]. Pool-boiling processes under vibration, shows that both the frequency and direction of vibration play crucial roles in heat-transfer outcomes[2)]. A 17 % improvement in heat transfer performance on a vibrating heated surface with spray cooling[3)]. Similarly, acoustic vibration can significantly enhance heat transfer in high-viscosity fluids[4)]. On further investigation of droplet dynamics on vibrating surfaces showed that vibration imparts additional inertial forces that help droplets overcome adhesive forces[5)], improving process efficiency[6)]. Marine heat exchangers subjected to vibration achieved remarkably 334 % increase in the Nusselt number as the vibration amplitude increased from 0 m to 3 m and the frequency from 0 Hz to 1 Hz[7)].

In parallel, advances in nanofluid technology have opened new possibilities for improving heat-transfer systems. The incorporation of nanoparticles modifies the fluid's

Cite: A. Tripure et al., "Entropy-Heat Transfer Coupling in Vibrational Non-Newtonian Nanofluid Flow with two phase study". Evergreen, 13 (02) 455-465 (2026). https://doi.org/10.5109/7420063.

thermophysical properties and enhances Brownian motion and thermophoretic effects, both of which contribute to increased convective efficiency. Even small concentrations of nanoparticles can significantly improve the thermal properties of the working fluid[8]. Nanofluids are now widely used in solar thermal devices, as working fluids in heat pipes and thermosyphons for compact electronic cooling, and even in biomedical applications such as nano-drug delivery systems using iron-based nanoparticles. In automotive radiators nanofluids improve thermal performance and allow for smaller radiator designs, which in turn benefit aerodynamic efficiency and overall vehicle performance[9]. The advanced studies have shown the impact of different rheological properties and boundary conditions effect on heat transfer and pressure drop[10].

The combination of vibration and nanofluids has been shown to further enhance convective heat transfer. The Reynolds number, nanoparticle size and concentration, and base-fluid type all strongly influence this combined effect. Numerical studies on non-Newtonian nanofluids subjected to vibration reported a maximum thermal-performance factor of 3.7[11]. The impact of in-plane and out-of-plane vibration on nanofluid flow in pipes and demonstrated significant improvements in heat-transfer characteristics using a three-dimensional dynamic model[12].

A deeper understanding of these phenomena is aided by thermal enhancement factor (TEF) and irreversibility analysis, first introduced by Bejan[13], which provides a second-law-based framework for assessing the irreversibilities in thermal systems. Temperature differences between fluid and pipe walls cause thermal irreversibilities, while viscous effects generate frictional losses, making entropy generation an essential measure of system inefficiency. With increasing demand for energy-efficient technologies, entropy analysis has become vital for optimizing heat-exchanger designs. Studies by[14] on smooth ducts and helically coiled tubes and by[15] on conical tubes show how Entropy Generation Analysis can guide the design of systems for reduced irreversibility and enhanced thermodynamic performance.

Numerical investigation shows effects of mechanical vibration on entropy generation in nanofluid flows. Their results revealed that vibration enhances heat transfer through intensified fluid agitation and particle dispersion, thereby reducing entropy generation particularly in non-Newtonian fluids at low Reynolds numbers[16]. Vibration was also found to induce swirling motion and radial mixing, which led to a more uniform temperature distribution nearly a hundred fold improvement compared to steady-flow conditions and in some cases increased heat-transfer coefficients by up to five times. These findings highlight that while vibration often boosts heat transfer, the associated thermodynamic efficiency depends on the balance between improved convection and any added irreversibility. Ultrasonication shows the enhancement in the heat transfer as well as the stabilility as it has beneficial effects of radial mixing, swirling motion as well as the stability improvement due to these effects[17].

This complexity is particularly important because adding nanoparticles not only raises thermal conductivity but also affects viscosity and flow resistance. A higher heat-transfer rate does not necessarily mean higher overall efficiency if accompanied by greater entropy production. Entropy-generation minimization thus provides a quantitative tool to evaluate such trade-offs and to design vibration-assisted nanofluid systems with optimal performance[18].

Beyond conventional experimental and numerical approaches, recent advances in computational methods have enriched the study of these complex systems. Fractional-derivative models analyzes CuO and Ag nanofluids with slip and mixed convection, highlighting how nanoparticle type and base-fluid properties affect flow and thermal fields. EMHD creeping flow of nanofluids in ciliated micro-channels, finding that Hartmann number, porosity, and cilia length significantly influence pressure drop and heat-transfer performance[19]. Peristaltic transport of chemically reactive Ellis fluids in asymmetric channels, shows that reaction kinetics and Schmidt number affect concentration fields[20], also micro-polar nanofluids with activation energy and nonlinear heat sources[21]. Hall and ion-slip effects in radiative second-grade fluids together with AI-assisted modeling of eco-friendly composite materials, advanced mathematical and data-driven methods are being integrated into thermal-fluid research[22].

Recent studies shows that incorporating nanofluids into photovoltaic–thermal (PV/T) systems can markedly improve both thermal and electrical performance by modifying their rheological and thermophysical properties[23]. Rising solar radiation and inlet temperatures elevated absorber and outlet fluid temperatures while reducing electrical efficiency, with thermal efficiency initially increasing before stabilizing[24]. Parallel studies emphasized stability as a key requirement, demonstrating that surfactants such as CTAB and tannic acid–ammonia can extend nanofluid life up to 93 days without significantly affecting density or viscosity. ZnO–water and Ag–water nanofluids further enhanced thermal performance, with ZnO at 12 wt% achieving up to 12.78% higher thermal efficiency. While electrical gains were modest, hybrid PV/T designs showed combined electrical and thermal enhancements of 8.5% and 18% respectively[25], with energy cost reductions of 82% and payback periods under two years[26].

Building upon this, hybrid PV/T–PCM systems demonstrated even stronger performance. Experimental use of ZnO–water (0.2 wt%) with paraffin wax PCM improved electrical output by 7–12% and raised thermal exergy by nearly 79% than conventional PV and

nanofluid-only PV/T. These systems achieved peak energy and exergy efficiencies of 65.7% and 13.6% while reducing entropy generation by 3.2%. A novel design integrating SiC–water nanofluid with nano-enhanced PCM reached 13.7% electrical and 72% thermal efficiency, generating 120.7 W power at a cost of 0.112 USD/kWh[27] and has a payback period of approximately 5 years[28]. Such hybridization confirms that the coupling of nanofluids with PCMs improves heat storage, regulates PV temperature, and enhances energy–exergy sustainability.

More recently, computational frameworks such as the Bilinear Neural Network Model (BNNM) and Bilinear Residual Neural Network (BRNM), inspired by the classical Hirota bilinear method[29], have been employed to solve nonlinear PDEs in vibrated thermal systems. These approaches can effectively capture turbulence, particle dispersion, and entropy-generation mechanisms [30]. Neuro-symbolic methods now merge neural-network learning with symbolic computation to identify closed-form expressions for entropy generation and flow fields, offering deeper physical insight and complementing traditional vibration-nanofluid studies[31].

Taken together, these developments show that mechanical vibration, especially when combined with nanofluids, is a powerful strategy for enhancing convective heat and mass transfer. By integrating entropy-generation analysis with advanced numerical and data-driven modeling techniques, researchers can design and optimize next-generation thermal systems for energy-efficient industrial, transportation, biomedical, and microscale applications.

This study employs computational fluid dynamics (CFD) to analyze the interplay between heat transfer enhancement, Themal Enhancement factor and irreversibility minimization in Non-Newtonian nanofluid flow under mechanical vibration. The influence of vibrational parameters is evaluated across constant wall temperature thermal boundary conditions to identify configurations that optimize performance based on both the first and second laws of thermodynamics. Through numerical simulations, the study explores how boundary conditions govern heat and entropy transport, emphasizing the role of vibration in improving thermal efficiency and reducing irreversibility. Notably, this work presents, for the first time, a detailed analysis of the trade-off between heat transfer and entropy generation in such vibrated nanofluid systems.

2. Numerical Procedure

The continuity, momentum and energy equations are solved using Volume of Fluid method using ANSYS Fluent 24 R1for simulation domain and are given below-

$$\frac{\partial \rho}{\partial t} + \nabla\left(\rho \vec{U}\right) = 0 \qquad (1)$$

$$\frac{\partial (\rho \vec{U})}{\partial t} + \nabla\left(\rho \vec{U}\vec{U}\right) = -\nabla p + \nabla\left[\mu\left(\nabla \vec{U} + \nabla \vec{U}^{T}\right)\right] + \rho \vec{g} + \vec{F}_s \qquad (2)$$

$$\frac{\partial (\rho C_p \nabla T)}{\partial t} + \nabla\left(\rho \vec{U} h\right) = \nabla(\lambda \nabla T) \qquad (3)$$

Thermo physical properties ρ, μ, C_p and λ, are fluid density, dynamic viscosity, heat capacity and thermal conductivity respectively of fluid. t is the time, $\vec{U}$ is the velocity vector, p is the pressure, $\vec{g}$ gravitational acceleration vector, $\vec{F}_s$ is the body force, h is the enthalpy and T is the temperature. Subscripts f and nf has been used for base fluid and nanofluids, respectively to describe the thermo physical properties as given in the table 1. In momentum equation (Eq.2), second term in right hand side is shear stress term which is denoted by τ_{ij} and given by

$$\tau_{ij} = \mu\left(\frac{\partial v_i}{\partial x_j} + \frac{\partial v_j}{\partial x_i} - \frac{2}{3}\mu\delta_{ij}\frac{\partial v_i}{\partial x_i}\right) \qquad (4)$$

The length of pipe (L) is 2m and radius(R) is 5mm. The simulation domain is shown in Figure 1. In solving these equations, appropriate boundary and initial conditions are specified based on the flow configuration and modeling assumptions. These are -

1) Inlet: To establish fully developed hydrodynamic conditions, a constant inlet velocity profile, $U_z = f(r,\theta,0) = contant$, was applied in both steady and vibrational flow simulations. The inlet velocity was evaluated using the Reynolds number expression, with a uniform inlet temperature fixed at T_i=293 K.
2) Outlet: Pressure outlet $P_o(r,\theta,1) = 0\ P$, zero-gauge pressure.
3) Wall: A uniform wall temperature T_w=*373K* was applied to the wall in both steady-state and vibrational flow simulations. To model vibration, the wall was subjected to a sinusoidal velocity in the x-direction, expressed as $v_{wall} = a2\pi f cos(2\pi f t)$thereby accounting for the oscillatory influence on the flow field.

Boundary motion was modeled by applying mesh deformation within the fluent module, allowing nodal displacement in the boundary region. A zero-gauge pressure was imposed at the external wall of the pipe to serve as the reference pressure under both flow regimes. Simulations were carried out over a Reynolds number range of 4000-14000 to examine the effects on temperature fields, radial mixing behavior, and heat-transfer performance. The residence time, defined as the time taken by the fluid to exit the pipe, was estimated based on the Reynolds number and pipe length. The temporal resolution was established by subdividing each oscillation period into 12 discrete intervals; for example, at 50 Hz (period = 0.2 s), the chosen time step was 1.6667×10^{-3} s.

Time steps were refined through preliminary testing, with a configuration of 12 iterations per step adopted for improved accuracy and efficiency. The solution was considered converged when the RMS residuals of the

Cite: A. Tripure et al., "Entropy-Heat Transfer Coupling in Vibrational Non-Newtonian Nanofluid Flow with two phase study". Evergreen, 13 (02) 455-465 (2026). https://doi.org/10.5109/7420063.

Table 1: Simulation Parameters

Sl.	Parameters	Range
1	Reynolds number	$Re = 4000 - 14000\ [-]$
2	Solid particle concentration	$\phi = 0 - 1.5\%\ [-]$
3	Frequency	$f = 25 - 100\ [Hz]$
4	Amplitude	$a = 2 - 4\ [mm]$
5	Constant wall temperature (WT)	$T_w = 373K$

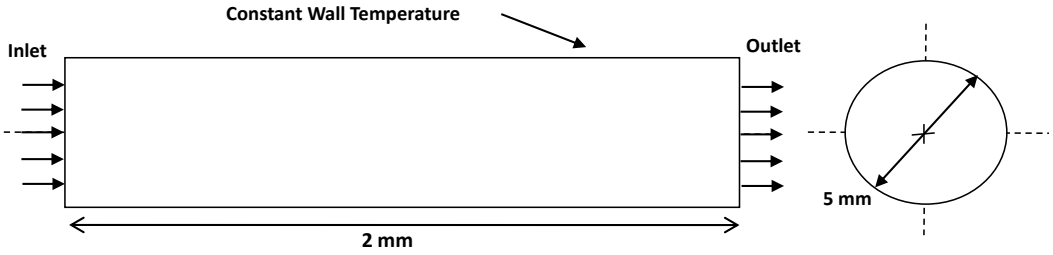

Fig. 1: Simulation domain

continuity, momentum, and energy equations fell below $10^{-}6$, and computations proceeded until the fluid residence time was achieved.

3. Data Reduction

The Nusselt number (Nu) is a dimensionless parameter that quantifies the efficiency of convective heat transfer between a fluid and a solid surface. It is defined as the ratio of the convective heat transfer coefficient to the thermal conductivity of the fluid, scaled by a characteristic length. Mathematically, it can be expressed as:

$$\boldsymbol{Nu} = \frac{\boldsymbol{hD_h}}{\boldsymbol{k}} \qquad (5)$$

Where h is the convective heat transfer coefficient in W/mK, $\boldsymbol{D_h}$ is the characteristic diameter in m and k is the thermal conductivity of the fluid in W/m^{2}K.
Nusselt number can also be expressed as

$$\boldsymbol{Nu} = \frac{\left(\frac{f}{8}\right)(\boldsymbol{Re}-\boldsymbol{1000})*\boldsymbol{Pr}}{\boldsymbol{1+12.7}*\left(\frac{f}{8}\right)^{\frac{1}{2}}*(\boldsymbol{Pr}^{\frac{2}{3}}-\boldsymbol{1})} \qquad (6)$$

Eq (6) is Gnielinski equation[32].
The heat transfer coefficient h is typically calculated based on the heat flux, surface area, and temperature difference, using:

$$\boldsymbol{h} = \frac{\boldsymbol{Q}}{\boldsymbol{A}(\boldsymbol{T_w}-\boldsymbol{T_f})} \qquad (7)$$

Where Q is the heat transferred in W, A is the surface area of heat transfer in m^2, $\boldsymbol{T_w}$ is the wall temperature in K, and $\boldsymbol{T_f}$ is the bulk mean fluid temperature in K.
Irreversibility (ϕ) is expressed as

$$\boldsymbol{\phi} = \frac{\boldsymbol{N_{s,vib}}}{\boldsymbol{N_{s,static}}} \qquad (8)$$

4. Grid Independency and Validation

To ensure the accuracy and reliability of the numerical model, a two-step approach was adopted during the numerical analysis. First, a grid-independency test was performed to confirm that the results were no longer dependent on mesh size or the number of elements. ICEM-CFD was used to generate a hexahedral grid over the domain.
For hydrodynamic validation, the pressure drop during water flow through a pipe at Reynolds number (Re) = 4000 was analyzed. Pr is the Prandtl number of the base fluid. The pressure drop from the simulation was compared with theoretical results based on the Hagen-Poiseuille equation as presented in Table 2.
Simulations were conducted using different edge divisions in both the cross-section and length of the pipe. It was observed that a grid size of 40 × 2000 (and beyond) provided results with minimal error, ensuring accuracy. This grid configuration was then used to validate heat-transfer performance.

$$Nu_z = 4.364 + 8.68\left(\frac{z}{DRePr}10^3\right)^{-0.506} exp^{\left(-41\frac{z}{DRePr}\right)} \qquad (9)$$

$$Pr = \frac{(C_p)_f \mu_f}{k_f} \qquad (10)$$

To validate heat transfer, the variation of the local Nusselt number along the pipe length was compared with Shah and London's equation for convective heat transfer in laminar flow (Eq. 8)[33], as shown in Figure 2. Two grid sizes, 35 × 1000 and 40 × 2000, 50 × 4000 were tested, all showing

Cite: A. Tripure et al., "Entropy-Heat Transfer Coupling in Vibrational Non-Newtonian Nanofluid Flow with two phase study". Evergreen, 13 (02) 455-465 (2026). https://doi.org/10.5109/7420063.

Table 2: Grid independence for Nusselt number

S No.	Number of Nodes/ 10^4	Average Nusselt Number	Percentage Error (%)
1	121.10	44.18	3.45
2	154.24	43.98	2.22
3	188.76	42.52	1.54
4	210.26	40.12	0.89
5	228.80	38.22	0.6

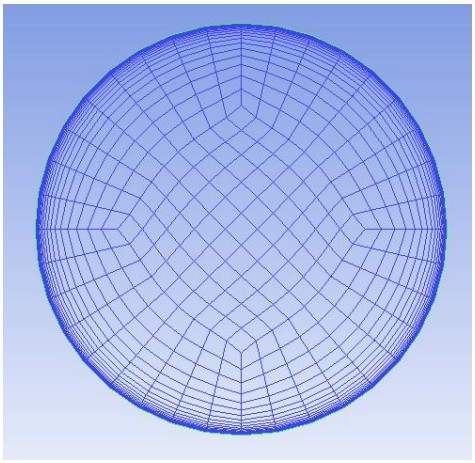

Fig. 2: Meshed cross-section vie of pipe

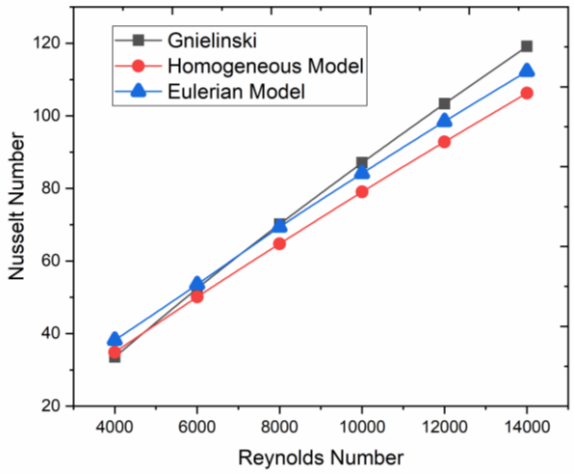

Fig. 3: Validation curve

high accuracy. Based on these results, a grid size of 40 × 2000, corresponding to approximately 22, 88,000 elements, was selected for the simulations.

5. Result and Discussion

5.1. Vibration-Induced Flow Modification and Sensitivity Analysis

In Figure 4, velocity contour maps are presented at the pipe exit for the three amplitudes employed. The Figure demonstrates how the velocity field evolves with changes in amplitude. The strong correlation between amplitude and radial mixing, which governs both temperature and velocity uniformity, can be attributed to the intensified fluid mixing induced at higher amplitudes.

This strong correlation affirms that the physical mechanisms—such as the impact of Reynolds number and vibration frequency on flow structure and heat transfer—have been accurately captured in the simulation. Hence, the validation confirms the model's robustness and its suitability for further analysis of nanofluid flow under vibrational effects, as shown in Figure 3.

Sensitivity analysis (Figure 5) was carried out for nanofluid flow through pipe at constant temperature condition. Reynolds number, particle concentration, frequency and amplitude of vibration were taken as input variable whereas heat transfer coefficient was considered as output variable. The analysis was performed with 50 simulation data set. Mathematical expression was generated by multiple regression model. Input variables for analysis were chosen by putting mean value of each parameter in the derived expression. Output parameter calculated by varying 20% of individual input parameters. It was found from the analysis that amplitude is the most influencing parameter and then frequency, Reynolds number and volume concentration in the simulation range.

5.2. Effect of vibration on Nusselt number

Figures 6(a), (b) and (c) illustrates the variation of the Nusselt number (Nu) across a range of Reynolds numbers (4,000 to 14,000) within the turbulent flow regime. It is clearly observed that increasing the vibration frequency leads to a consistent rise in the Nusselt number, indicating enhanced convective heat transfer. Furthermore, on increasing the amplitude of vibration from 2 mm to 4 mm, results in a more pronounced increase in Nu, emphasizing the role of vibration in promoting thermal transport.

Further insights are provided, which depict the relationship between Nu and vibration amplitude at fixed Reynolds numbers of 4,000, 10,000 and 14,000. In the static case (no vibration) at Re = 4,000, the Nusselt number is 38.22, which increases to 224.34 when the amplitude is raised to 4 mm at 100 Hz. At Re = 10,000, Nu rises from 86.83 (static) to 202.99 under the same vibration conditions. At Re = 14,000, Nu rises from 118.24 (static) to 224.34 under the same vibration conditions, as shown in Figure 8b. Similarly, Figure 8c demonstrates that at Re = 14,000, Nu increases from 118.24 in the static case to 224.34 at the highest amplitude and frequency applied. These findings collectively demonstrate that vibration significantly enhances the convective heat transfer, especially at higher Reynolds numbers and more intense vibration conditions.

The observed enhancement in convective heat transfer resulting from vibration can be primarily attributed to three key mechanisms: enhanced fluid mixing, disruption of the thermal boundary layer, and increased turbulence intensity within the flow domain.

Cite: A. Tripure et al., "Entropy-Heat Transfer Coupling in Vibrational Non-Newtonian Nanofluid Flow with two phase study". Evergreen, 13 (02) 455-465 (2026). https://doi.org/10.5109/7420063.

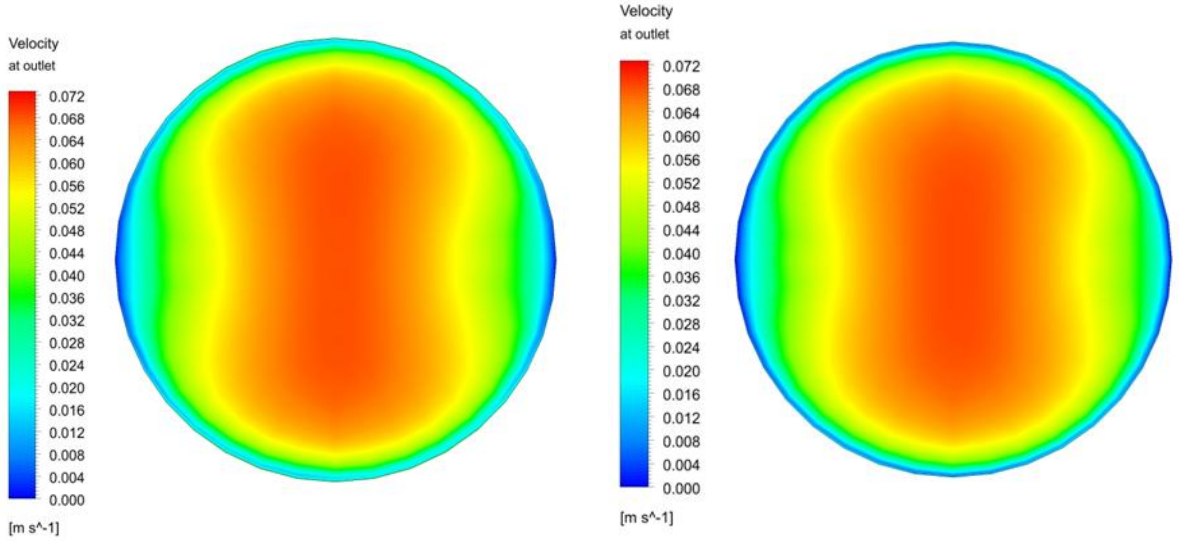

(a) a=2mm (b) a=3mm

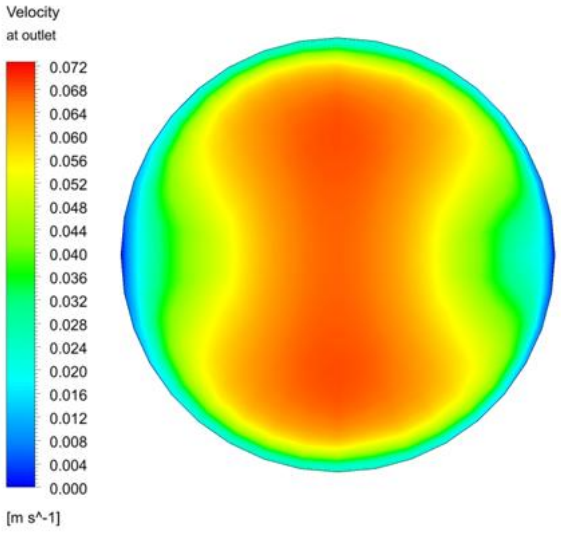

(c) a=4mm

Fig. 4: Velocity contour maps at different vibration amplitude
$\mathbf{T_w = 373K; T_i = 293K; f = 25\ Hz; Re = 4000; \varphi = 1.5}$ %.s

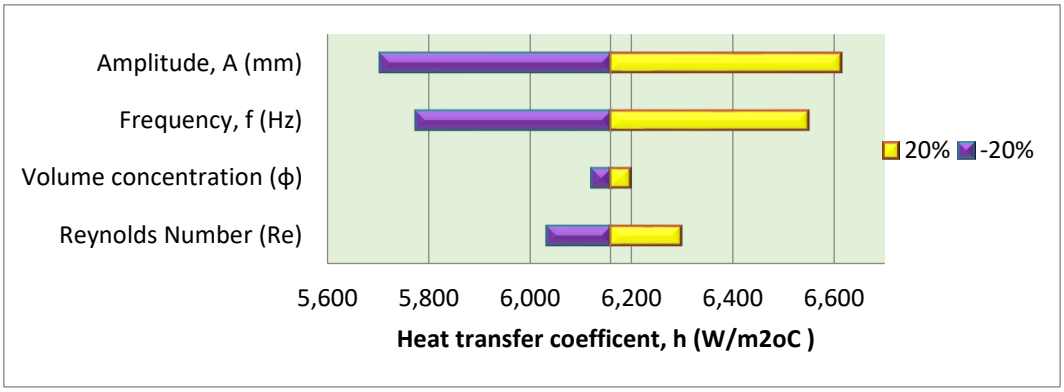

Fig. 5: Sensitivity analysis: $D = 5\ mm; L = 2000\ mm;$ Tw = 373K; Ti = 293K

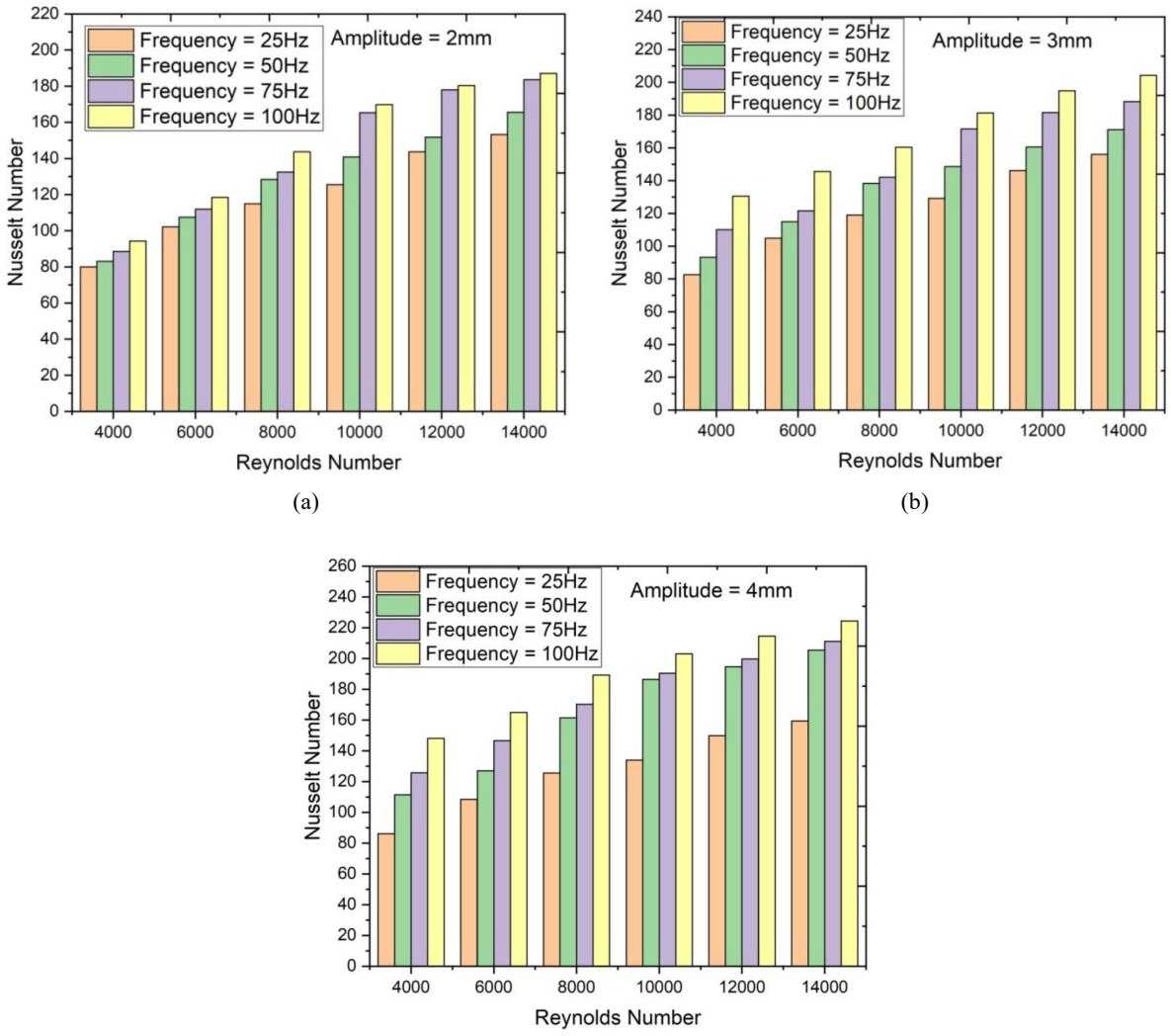

Fig. 6: Nu vs. Re for various frequencies of vibration at amplitude (a) 2 mm, (b) 3 mm and (c) 4mm

5.3. Irreversibility

The Figure depicts the influence of vibration frequency on irreversibility at various Reynolds numbers. Irreversibility, which arises primarily from viscous dissipation and thermal gradients, is closely linked to the nature of the flow and the mixing behavior within the domain. At lower Reynolds numbers, the flow is more orderly motion, and irreversibility is dominated by thermal conduction due to less mixing and weaker momentum transport. As the Reynolds number increases, enhanced inertial effects promote stronger mixing and thinner thermal boundary layers, which can increase temperature gradients and therefore higher thermal irreversibility.

The application of vibration introduces time dependent disturbances that alter the flow structure by inducing oscillatory motion and promoting secondary flow development. These effects minimizes with increasing frequency and amplitude. The results indicate that higher vibration amplitudes, especially at intermediate to high Reynolds numbers, significantly reduce irreversibility. This is attributed to the enhanced mixing and disruption of thermal and velocity boundary layers, which reduces both thermal and viscous sources of irreversibility.

At a Reynolds number of 6000 and amplitude of 2 mm, increasing the vibration frequency from 25 Hz to 100 Hz reduces the irreversibility from 0.96 to 0.81. Similarly, increasing the amplitude from 2 mm to 4 mm reduces the irreversibility from 0.96 to 0.76 at 25 Hz and from 0.81 to 0.45 at 100 Hz, indicating that higher vibration frequency and amplitude collectively contribute to lower exergy destruction under these conditions. On increasing the Reynolds number the irreversibility increases. Thus, the interaction between vibration frequency and Reynolds number plays a critical role in modulating the entropy generation characteristics, with higher amplitudes yielding more thermodynamically favorable conditions as shown in Figure 7 (a), (b) and (c).

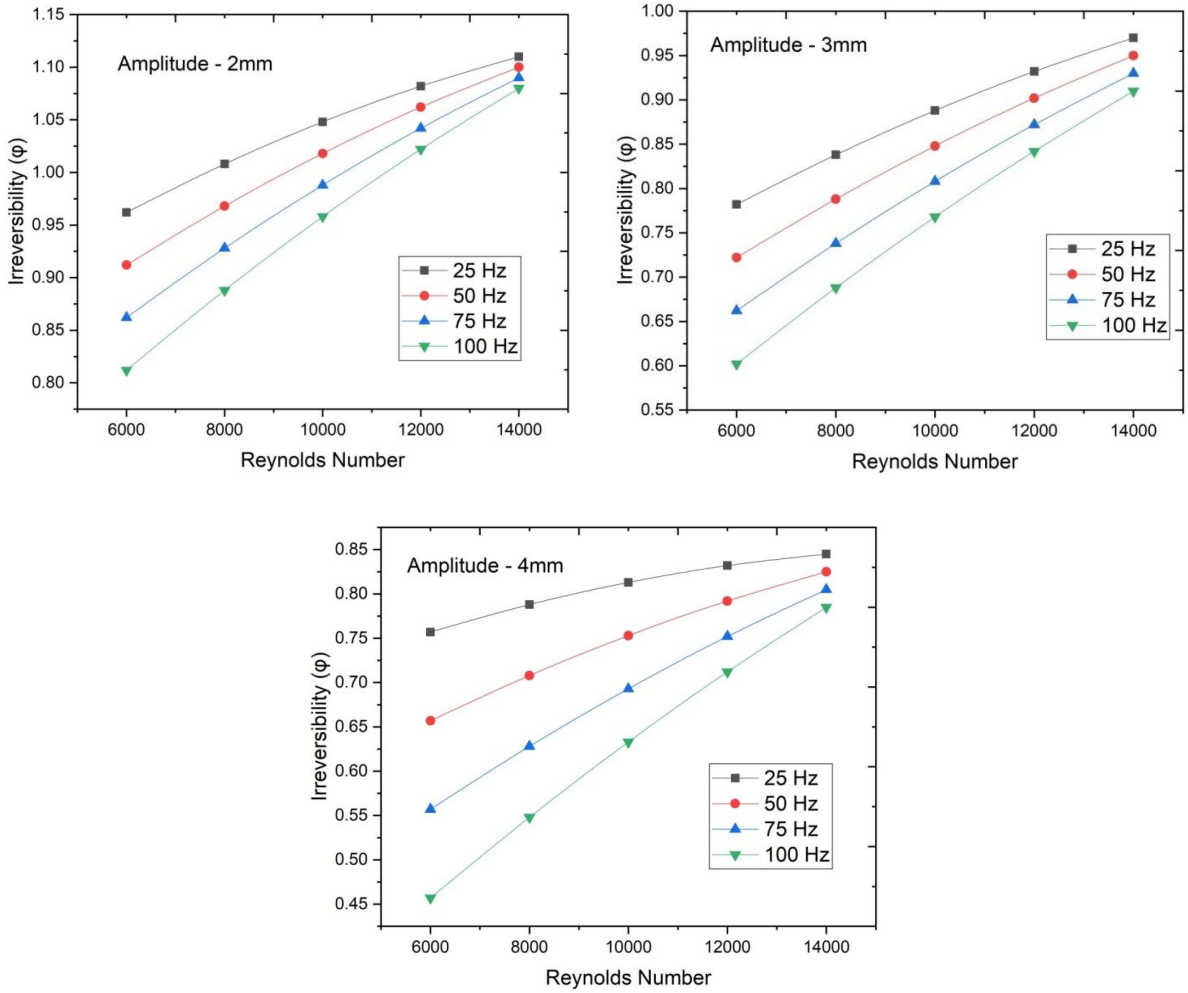

Fig. 7: Irreversibility vs. Reynolds number for different frequency amplitude (a) 2mm, (b) 3mm, and (c) 4mm

5.4. Effect of Vibration Intensity on Entropy Generation

Entropy generation is the measure of irreversibility of the thermal system. More irreversible system implies more entropy generation. The entropy generation of a system is the combined effects of thermal as well as frictional factor. In this case, increasing vibration intensity, characterized by frequency and amplitude, modifies the balance between thermal and viscous contributions to entropy generation. At relatively low amplitudes and higher frequencies, vibration enhances fluid mixing and disrupts the thermal boundary layer, thereby reducing temperature gradients and suppressing thermal entropy generation. This reflects the beneficial role of vibration in augmenting convective transport and lowering irreversibility associated with heat transfer. With increasing amplitude, however, stronger oscillatory motion introduces larger velocity fluctuations and shear stresses. While such disturbances promote mixing, they also enhance viscous dissipation, raising the frictional component of entropy generation. As a result, higher amplitudes often offset the thermal benefits by generating additional irreversibility. This interplay leads to distinct trends: entropy generation declines more steeply with Reynolds number under low-amplitude, high-frequency conditions, while higher amplitudes tend to flatten this variation, especially at lower frequencies. Thus, optimum conditions for minimizing entropy are typically achieved at moderate amplitudes and relatively high frequencies, where enhanced mixing suppresses thermal gradients without inducing excessive viscous losses.

These interpretations align with the findings of[34], which emphasize the dual influence of vibration on thermal and viscous fields, and with the recent work of[35], who demonstrated that vibration-induced nanofluid flows exhibit a non-monotonic entropy response, confirming that carefully tuned vibrational parameters can suppress irreversibility while improving heat transfer.

6. Conclusion

This study demonstrates that mechanical vibration significantly influences both heat transfer performance and entropy generation in non-Newtonian nanofluid flows. The introduction of vibrational motion enhances radial mixing, leading to improved temperature uniformity and increased

heat transfer, under constant wall temperature conditions. Sensitivity analysis identifies amplitude as the most dominant parameter, followed by frequency, Reynolds number, and nanoparticle concentration. Importantly, the entropy generation analysis reveals that while vibration enhances mixing, it also modifies the distribution of thermodynamic irreversibility. Vibrational flow reduces entropy generation by flattening temperature gradients; however, excessive vibration can increase viscous dissipation, resulting in a rise in total entropy. This interplay suggests that optimal performance lies in balancing enhanced heat transfer with minimized entropy production. Two-phase models provide a more accurate representation of nanofluid behavior by capturing critical physical phenomena such as nanoparticle slip, diffusion, and clustering, which significantly influence local heat transfer. Two-phase simulations align more closely with experimental data than single-phase models, making them essential for the reliable design and optimization of nanofluid-based thermal systems, particularly under vibrational conditions.

Some of the important conclusions are mentioned below-

1. Across all Reynolds numbers, an increase in vibration amplitude leads to a consistent rise in the Nusselt number, indicating enhanced fluid mixing and turbulence. At 4 mm amplitude and 100 Hz, Nu increases from approximately 38–118 under static conditions to 202–224, confirming that higher vibration amplitudes significantly strengthen convective heat transfer performance.

2. Influence of frequency: A noticeable rise in heat transfer was observed with increasing frequency up to a certain level, beyond which the rate of enhancement tended to stabilize. Frequencies in the range of 25-100 Hz generally produced optimal enhancement across all cases. The effect of frequency on heat transfer was more pronounced at the higher amplitude. Frequencies between 25-100 Hz showed optimal enhancement, particularly in the 4 mm amplitude case. At low amplitude (2 mm), the influence of frequency followed a similar trend.

3. Irreversibility behavior: At Re = 6,000 and amplitude = 2 mm, increasing the frequency from 25 Hz to 100 Hz decreases irreversibility from 0.96 to 0.81. Raising the amplitude from 2 mm to 4 mm further reduces it to 0.76 at 25 Hz and 0.45 at 100 Hz. However, irreversibility generally increases with Reynolds number.

4. Entropy generation characteristics: Entropy generation, representing total system irreversibility, arises from both thermal and frictional effects. Increasing vibration intensity modifies the balance between these contributions: Low amplitudes and high frequencies enhance fluid mixing, suppress temperature gradients, and lower thermal entropy generation. High amplitudes introduce stronger velocity fluctuations and shear stresses, increasing viscous dissipation. Therefore, optimal conditions for minimizing entropy occur at moderate amplitudes and relatively high frequencies, where improved mixing enhances heat transfer without excessive viscous losses.

Future work should focus on the multi-objective optimization of vibrational parameters to achieve ideal trade-offs between heat transfer and entropy. Additionally, exploring advanced nanofluids like hybrid suspensions, validating models through experimentation, and extending the framework to turbulent and more complex geometries will broaden the applicability of this approach in industrial and engineering domains.

Acknowledgements

The authors confirm contribution to the paper as follows: Conceptualization, Data curation: Amrita Tripure and Santosh Kumar Mishra; Software: Amrita Tripure; Validation and review: Amrit Shende and Pushpendra Singh. All authors reviewed the results and approved the final version of the manuscript.

References

1) J. Fu, X. Miao, Q. Zuo, H. Tang, Y. Li, Y. Zhang, and B. Sunden, “Heat transfer and field synergy characteristics in a rectangular unit channel under mechanical vibration,” Int. Commun. Heat Mass Transf., 136 (June) 106176 (2022). doi:10.1016/j.icheatmasstransfer.2022.106176.

2) Y. Zhao, H. Wu, and C. Dang, “Effect of mechanical vibration on heat and mass transfer performance of pool boiling process in porous media: a literature review,” Front. Energy Res., 11 (November) 1–18 (2023). doi:10.3389/fenrg.2023.1288515.

3) X. Chen, A. Du, Z. Li, K. Liang, X. Wang, M. Zhang, and Y. Wang, “Heat transfer of single-phase spray cooling on heated vibrating surfaces,” Case Stud. Therm. Eng., 50 (September) 103489 (2023). doi:10.1016/j.csite.2023.103489.

4) X. Bin Zhan, Y.W. Zhang, and Y.L. Jiang, “Application of acoustic vibration promotes heat transfer of high-viscosity fluid in a container,” Numer. Heat Transf. Part A Appl., 1–18 (n.d.). doi:10.1080/10407782.2023.2290082.

5) X. Zhan, B. Ye, B. Li, and T. Shi, “Continuous conveying and mixing characteristics of high-viscosity materials under acoustic vibration excitation,” AIChE J., 70 (6) (2024). doi:10.1002/aic.18406.

6) X. Chen, A. Du, X. Wang, C. Yang, K. Liang, Z. Li, H. Zhou, and M. Zhang, “The effect of vibration on droplet dynamics and heat transfer of spray cooling,” Appl. Therm. Eng., 238 122074 (2024). doi:https://doi.org/10.1016/j.applthermaleng.2023.122074.

7) Y. Wang, S. Ding, A. Yan, H. Miao, F. Wang, and J. Yuan, “Flow and heat transfer performance analysis of brazed plate heat exchangers under marine vibration conditions,” Int. J. Therm. Sci., 205 109270

(2024). doi:https://doi.org/10.1016/j.ijthermalsci.2024.109270.

8) Z. Guo, "A review on heat transfer enhancement with nanofluids," J. Enhanc. Heat Transf., 27 (1) 1–70 (2020). doi:10.1615/JEnhHeatTransf.2019031575.
9) A.H. Alami, M. Ramadan, M. Tawalbeh, S. Haridy, S. Al Abdulla, H. Aljaghoub, M. Ayoub, A. Alashkar, M.A. Abdelkareem, and A.G. Olabi, "A critical insight on nanofluids for heat transfer enhancement," Sci. Rep., 13 (1) 1–14 (2023). doi:10.1038/s41598-023-42489-0.
10) S.K. Mishra, A. Tripure, A. Mishra, and P. Singh, "Effects of vibrational flow on nanofluid flow behavior under different temperature boundary conditions," Numer. Heat Transf. Part A Appl., 86 (17) 6206–6222 (2025). doi:10.1080/10407782.2024.2340071.
11) M.G.P. Kumar, B.G. Rao, B. Sreenivasulu, and S.S. Arasavelli, "Effect of vibration on heat transfer to laminar non-newtonian nanofluid flowing through a circular pipe: a numerical analysis," Numer. Heat Transf. Part A Appl., 82 (11) 683–699 (2022). doi:10.1080/10407782.2022.2083862.
12) J.-R. Yuan, and H. Ding, "Three-dimensional dynamic model of the curved pipe based on the absolute nodal coordinate formulation," Mech. Syst. Signal Process., 194 110275 (2023). doi:https://doi.org/10.1016/j.ymssp.2023.110275.
13) A. Bejan, "Second law analysis in heat transfer," Energy, 5 (8) 720–732 (1980). doi:https://doi.org/10.1016/0360-5442(80)90091-2.
14) R. Prattipati, V.K. Narla, and S. Pendyala, "Effect of viscosity on entropy generation for laminar flow in helical pipes," J. Therm. Eng., 7 (5) 1100–1109 (2021). doi:10.18186/thermal.977960.
15) A. Kaood, A. Aboulmagd, and A. ElDegwy, "Entropy generation analysis of turbulent flow in conical tubes with dimples: a numerical study," J. Therm. Anal. Calorim., 148 (12) 5667–5685 (2023). doi:10.1007/s10973-023-12127-y.
16) S.K. Mishra, A. Mishra, P. Singh, and M. Dubey, "Heat transfer and entropy generation in vibrational flow: newtonian vs. inelastic non-newtonian fluid," J. Appl. Fluid Mech., 17 (11) 2349–2360 (2024). doi:10.47176/jafm.17.11.2699.
17) M. Sandhya, D. Ramasamy, K. Sudhakar, K. Kadirgama, and W.S.W. Harun, "Ultrasonication an intensifying tool for preparation of stable nanofluids and study the time influence on distinct properties of graphene nanofluids – a systematic overview," Ultrason. Sonochem., 73 105479 (2021). doi:10.1016/j.ultsonch.2021.105479.
18) M. Vahabzadeh Bozorg, and M. Siavashi, "Two-phase mixed convection heat transfer and entropy generation analysis of a non-newtonian nanofluid inside a cavity with internal rotating heater and cooler," Int. J. Mech. Sci., 151 842–857 (2019). doi:10.1016/j.ijmecsci.2018.12.036.
19) O. Bafakeeh, A. Raza, S. Khan, M. Khan, A. Nasr, N. ben khedher, and S. Eldin, "Physical interpretation of nanofluid (copper oxide and silver) with slip and mixed convection effects: applications of fractional derivatives," Appl. Sci., 12 10860 (2022). doi:10.3390/app122110860.
20) A. Abbasi, S.U. Khan, W. Farooq, F.M. Mughal, M. Ijaz Khan, B.C. Prasannakumara, M.T. El-Wakad, K. Guedri, and A.M. Galal, "Peristaltic flow of chemically reactive ellis fluid through an asymmetric channel: heat and mass transfer analysis," Ain Shams Eng. J., 14 (1) 101832 (2023). doi:https://doi.org/10.1016/j.asej.2022.101832.
21) Y.-X. Li, U.F. Alqsair, K. Ramesh, S.U. Khan, and M.I. Khan, "Nonlinear heat source/sink and activation energy assessment in double diffusion flow of micropolar (non-newtonian) nanofluid with convective conditions," Arab. J. Sci. Eng., 47 (1) 859–866 (2022). doi:10.1007/s13369-021-05692-7.
22) V.V.L. Deepthi, M.M.A. Lashin, N. Ravi Kumar, K. Raghunath, F. Ali, M. Oreijah, K. Guedri, E.S.M. Tag-ElDin, M.I. Khan, and A.M. Galal, "Recent development of heat and mass transport in the presence of hall, ion slip and thermo diffusion in radiative second grade material: application of micromachines," Micromachines, 13 (10) (2022). doi:10.3390/mi13101566.
23) Y. Khanjari, F. Pourfayaz, and A.B. Kasaeian, "Numerical investigation on using of nanofluid in a water-cooled photovoltaic thermal system," Energy Convers. Manag., 122 263–278 (2016). doi:https://doi.org/10.1016/j.enconman.2016.05.083.
24) Y. Khanjari, A.B. Kasaeian, and F. Pourfayaz, "Evaluating the environmental parameters affecting the performance of photovoltaic thermal system using nanofluid," Appl. Therm. Eng., 115 178–187 (2017). doi:https://doi.org/10.1016/j.applthermaleng.2016.12.104.
25) A.H.A. Al-Waeli, M.T. Chaichan, H.A. Kazem, and K. Sopian, "Evaluation and analysis of nanofluid and surfactant impact on photovoltaic-thermal systems," Case Stud. Therm. Eng., 13 100392 (2019). doi:https://doi.org/10.1016/j.csite.2019.100392.
26) M.O. Lari, and A.Z. Sahin, "Design, performance and economic analysis of a nanofluid-based photovoltaic/thermal system for residential applications," Energy Convers. Manag., 149 467–484 (2017). doi:https://doi.org/10.1016/j.enconman.2017.07.045.
27) A.H.A. Al-Waeli, H.A. Kazem, M.T. Chaichan, and

K. Sopian, “Experimental investigation of using nano-pcm/nanofluid on a photovoltaic thermal system (pvt): technical and economic study,” Therm. Sci. Eng. Prog., 11 213–230 (2019). doi:https://doi.org/10.1016/j.tsep.2019.04.002.

28) M. Hosseinzadeh, M. Sardarabadi, and M. Passandideh-Fard, “Energy and exergy analysis of nanofluid based photovoltaic thermal system integrated with phase change material,” Energy, 147 636–647 (2018). doi:https://doi.org/10.1016/j.energy.2018.01.073.
29) M.A. Isah, A. Yokus, and D. Kaya, “BILINEAR neural network method for obtaining the exact analytical solutions to nonlinear evolution equations and its application to kdv equation,” Khayyam J. Math., 10 (2) 228–248 (2024). doi:10.22034/kjm.2024.396918.2865.
30) R.F. Zhang, and M.C. Li, “Bilinear residual network method for solving the exactly explicit solutions of nonlinear evolution equations,” Nonlinear Dyn., 108 (1) 521–531 (2022). doi:10.1007/s11071-022-07207-x.
31) J.-G. Liu, W.-H. Zhu, Y.-K. Wu, and G.-H. Jin, “Application of multivariate bilinear neural network method to fractional partial differential equations,” Results Phys., 47 106341 (2023). doi:10.1016/j.rinp.2023.106341.
32) V. Gnielinski, “New equations for heat and mass transfer in the turbulent flow in pipes and channels,” NASA STI/Recon Tech. Rep. A, 41 (1) 8–16 (1975).
33) R.K. Shah, and A.L. London, “Laminar Flow Forced Convection in Ducts: A Source Book for Compact Heat Exchanger Analytical Data,” Academic Press, 1978.
34) Y. Yang, H. Chen, X. Zou, X.L. Shi, W. Di Liu, L. Feng, G. Suo, X. Hou, X. Ye, L. Zhang, C. Sun, H. Li, C. Wang, and Z.G. Chen, “Flexible carbon-fiber/semimetal bi nanosheet arrays as separable and recyclable plasmonic photocatalysts and photoelectrocatalysts,” ACS Appl. Mater. Interfaces, 12 (22) 24845–24854 (2020). doi:10.1021/acsami.0c05695.
35) S.K. Mishra, A. Shende, A. Mishra, and P. Singh, “Exploring heat transfer augmentation and entropy generation in nanofluid flow induced by vibration: influence of velocity and rheological properties,” Numer. Heat Transf. Part A Appl., 0 (0) 1–18 (2024). doi:10.1080/10407782.2024.2381619.